

Measurement trajectories of chaotic quantum systems

M. Schlautmann and R. Graham

Fachbereich Physik, Universität GH Essen, D 45117 Essen, Germany

(Received 12 January 1995)

We consider the behavior of a classically chaotic quantum system, the periodically driven pendulum, under the influence of a continuous measurement of its angular momentum. Without measurement the system shows dynamical localization, a quantum interference effect that suppresses the classical chaotic diffusion in momentum space. The coupling of the system to a measuring device destroys its coherence and thus leads to delocalization. This is studied on the level of individual systems including the recording of the measurement results. For that purpose we analyze the appropriate stochastic Schrödinger equation, from which a stochastic quantum map is derived as an effective tool for numerical simulation of measurement trajectories. We show that a continuous momentum measurement restores the diffusive behavior of the system in momentum space, but that for sufficiently low accuracy of measurement the corresponding diffusion constant is smaller than the classical one. This is reflected by an equal diffusive growth of the recorded measurement results. Thus we find signatures of the classical chaos and of the dynamical localization both in the behavior of the measured quantum system and in the corresponding signal of the measuring device.

PACS number(s): 05.45.+b, 06.30.Gv

I. INTRODUCTION

The problem of quantum chaos can be characterized as the search for signatures of classical chaos in the behavior of the corresponding quantized systems [1]. Because of the correspondence principle they should appear in the quasiclassical regime, where Planck's constant is small compared to typical actions of the system. The usual point of view in this context is to consider the isolated quantum system, i.e., its eigenenergies and dynamics. However, in physical reality it is difficult to find such systems: In the quasiclassical regime the coupling of the system to a macroscopic environment becomes important and this can alter the quantum dynamics of the system qualitatively, especially in the case of classical chaos; it then behaves, in some sense, more classically [2–5].

A special and, from the experimental point of view, important kind of a macroscopic environment is a measuring device (henceforth called "meter"). Since classical chaos is studied by analyzing continuously observed trajectories of the system [6], it is also natural to investigate the dynamics of the continuously measured quantum system and the received measurement results. This involves the problem of quantum measurement [7,8], i.e., the derivation of the irreversible "reduction of the wavefunction" from the unitary evolution of the total system comprising the observed system (simply called "system" in the following) and the meter. But it provides a conceptionally new approach to the "search for quantum chaos."

Perhaps the most important physical effect in the quantum dynamics of classically chaotic systems is "dynamical localization." It is a variant of the Anderson localization of electrons in disordered media [9,10] and therefore based on destructive interference of waves in random systems. But in dynamical localization the randomness is not imposed externally, but produced dynam-

ically by a simple and completely deterministic dynamical system. According to theory [11] this effect should appear, under appropriate conditions, in periodically driven chaotic quantum systems. After a certain time it suppresses the classically observed diffusive increase of the action variable, which then shows quasiperiodic fluctuations around a definite mean value of its variance. Dynamical localization has been discussed theoretically for model systems such as the kicked rotor [12–14], atomic [15] and molecular [16] models, Josephson junctions [17], and quantum optical examples [18,19]. Furthermore, there is experimental evidence that it occurs in hydrogen atoms in Rydberg states driven by a strong microwave field [20,21]. Very recently there have been attempts to observe dynamical localization in atomic momentum transfer by a modulated standing light wave [22]. The latter is a quantum optical realization of a periodically driven pendulum [18]. Another possible realization of this system is provided by a current-driven Josephson junction [17].

In the present paper we wish to study the effect of a continuous measurement on dynamical localization. We shall consider as a concrete and experimentally relevant example a continuous angular momentum measurement for the driven quantum pendulum and study its influence on the dynamical localization of the system. Since the localization effect rests entirely on quantum coherence, which will be disturbed by the coupling to a meter, it is expected that some mechanism of delocalization will set in. Previous studies of the delocalization effect were performed for the kicked rotor coupled to a macroscopic environment [4] or to a meter [5], however, without any attempt to correlate the delocalization with the received signal of the meter. The main purpose in the present paper is to study the mechanism of delocalization for an individually measured driven pendulum including the way in which delocalization is reflected in the recorded

measurement results. This enables us to discern the signatures of classical chaos, on the one hand, and of dynamical localization, on the other hand, in the behavior of the measured quantum system and in the corresponding signal of the meter.

In the following section we present the basic tool we shall use, the description of continuously measured individual systems by a stochastic Schrödinger equation. This tool was developed from phenomenological theories of the dynamical reduction of the wave function [23–27], which recently could be deduced from an idealized microscopic model of a Markovian meter [28–30]. For a momentum measurement of periodically kicked systems we derive a stochastic quantum map, which can be implemented simply on a computer to simulate the (conditional) evolution of the state vector of the measured system (referring to a certain realization of the measurement signal); we will call such a conditional quantum evolution a “measurement trajectory of the system.” Furthermore, we show how the measurement results are connected with the system observables. Section III deals with the isolated behavior of the periodically driven pendulum, i.e., with the conditions and quantitative description of its classical chaos and the corresponding dynamical localization. In Sec. IV we then analyze in detail the quantum trajectories of the system under angular momentum measurement and in Sec. V we summarize our conclusions.

II. MEASUREMENT TRAJECTORIES OF INDIVIDUAL QUANTUM SYSTEMS

In contrast to the classical case, the influence of measurements cannot be neglected for quantum systems. Rather the backaction of a measuring device has to cause a stochastic and nonunitary change of the system state vector, which is often called the “reduction of the wavefunction.” This requires an effective classical behavior of the meter and the deduction of such a classical meter from a microscopic quantum model is the task in the quantum measurement problem [7,8].

A. Stochastic Schrödinger equation

Recently it has been shown [28–30] that the linear coupling of the system to an idealized Markovian meter, consisting of a Bose field in a state of quantum white noise [31], leads to a stochastic Schrödinger equation for the time evolutions of the individual system conditioned by the received measurement results. It is the singular coupling between the system and the Bose field that causes a self-commutative evolution of the recorded meter observable [28] and thereby provides an effective classical behavior of the meter, i.e., a solution of the measurement problem. The resulting stochastic Schrödinger equation for a continuous measurement of the observable A of a system with the Hamiltonian H_S can be written down in essentially two ways. In its linear version it describes the time evolution of an unnormalized state vector $|\phi(t)\rangle$ and has in Ito form the structure

$$d|\phi(t)\rangle = \left(-\frac{i}{\hbar} H_S - \frac{\gamma}{4} A^2 \right) |\phi(t)\rangle dt + A |\phi(t)\rangle d\xi(t), \quad (1)$$

where ξ is an effective classical Wiener process with $[d\xi(t)]^2 = (\gamma/2)dt$ [28–30]. However, in this version the probability measure one has to use for the process ξ to compute physical mean values is not just the Wiener measure $dP_t^W[\xi]$, but the measure

$$dP_t[\xi] = dP_t^W[\xi] \langle \phi(t) | \phi(t) \rangle, \quad (2)$$

where $\langle \phi(t) | \phi(t) \rangle$ is a functional of $d\xi(t')$ for $t' < t$. The equivalent stochastic Schrödinger equation for the normalized state $|\psi(t)\rangle = |\phi(t)\rangle / \sqrt{\langle \phi(t) | \phi(t) \rangle}$ with a probability for its stochastic realization that is given by the usual Wiener measure of the involved Wiener process has the nonlinear form

$$d|\psi(t)\rangle = \left(-\frac{i}{\hbar} H_S - \frac{\gamma}{4} [A - \langle A(t) \rangle]^2 \right) |\psi(t)\rangle dt + [A - \langle A(t) \rangle] |\psi(t)\rangle d\xi(t), \quad (3)$$

where $\langle A(t) \rangle = \langle \psi(t) | A | \psi(t) \rangle$ [28–30]. Each realization of the Wiener process ξ is connected with a measurement trajectory of the system — represented by a corresponding solution $|\psi\rangle$ of the above equation — and with a realization of the recorded measurement results \mathcal{A} . The latter can be received from the former via

$$\mathcal{A}(t) dt = \langle A(t) \rangle dt + \frac{1}{\gamma} d\xi(t) \quad (4)$$

[28–30]. Hence the parameter γ , which is proportional to the strength of the coupling between the system and the meter, determines the measurement accuracy; the higher the value of γ the better the accordance between \mathcal{A} and $\langle A \rangle$. We will see below that an increase of γ also results in a stronger reduction of the wave function.

If one disregards (i.e., averages over) the recorded measurement results the system state is described by the statistical operator $\bar{\rho}(t) := \langle \bar{\psi}(t) | \langle \psi(t) \rangle \rangle$, where the bar denotes the average with respect to the involved Wiener process. It satisfies the master equation

$$\frac{d\bar{\rho}(t)}{dt} = -\frac{i}{\hbar} [H_S, \bar{\rho}(t)] - \frac{\gamma}{4} [A, [A, \bar{\rho}(t)]]. \quad (5)$$

B. Application to periodically kicked systems

In view of the computational effort in analyzing chaotic quantum dynamics it is advantageous to consider one-dimensional periodically kicked systems, i.e., systems with a Hamiltonian

$$H_S = \frac{p^2}{2} + V(\theta, t) \sum_{j=-\infty}^{\infty} \delta(t/\tau - j). \quad (6)$$

p and θ are the (rescaled) dimensionless momentum and position variables, respectively, and satisfy the canonical commutation relation

$$[p, \theta] = -i\hbar, \quad (7)$$

where \hbar denotes the rescaled Planck constant. The Schrödinger equation of the system can be integrated over a time interval of one kicking period. This yields the quantum map

$$\begin{aligned} |\psi(j+1)\rangle &= U_\tau |\psi(j)\rangle \\ &:= \exp\left(-\frac{i}{\hbar} \frac{p^2}{2\tau}\right) \exp\left(-\frac{i}{\hbar} V(\theta, j)\right) |\psi(j)\rangle \end{aligned} \quad (8)$$

with the abbreviation $f(j) := f(j\tau - \epsilon)$, $\epsilon \searrow 0$.

If now the meter described above is coupled to a system observable $A(p)$, which commutes with the momentum p , the linear version of the stochastic Schrödinger equation (1) can also be integrated over one kicking period. Thereby (cf. the Appendix) one obtains a stochastic quantum map for the corresponding normalized state vector $|\psi\rangle$ of the form

$$\begin{aligned} |\psi(j+1)\rangle &= \frac{(\frac{\alpha}{\pi})^{1/4} \exp[-\frac{\alpha}{2}(A - \tilde{A}(j+1))^2]}{\sqrt{p(\tilde{A}(j+1))}} \\ &\quad \times U_\tau |\psi(j)\rangle. \end{aligned} \quad (9)$$

Here $\alpha := \gamma\tau$ and

$$\tilde{A}(j+1) := \frac{1}{\tau} \int_{j\tau-\epsilon}^{(j+1)\tau-\epsilon} A(t) dt, \quad \epsilon \searrow 0 \quad (10)$$

is a random variable with the probability density

$$\begin{aligned} p(\tilde{A}(j+1)) &= \sqrt{\frac{\alpha}{\pi}} \langle \psi'(j+1) | \\ &\quad \times \exp\left[-\alpha(A - \tilde{A}(j+1))^2\right] |\psi'(j+1)\rangle, \end{aligned} \quad (11)$$

where $|\psi'(j+1)\rangle := U_\tau |\psi(j)\rangle$. So the continuous A recording acts like a repeated A measurement with frequency $1/\tau$. The corresponding results are given by the time averages of the A signal with respect to the preceding kicking period and their accuracy is described by the parameter α .

Equation (9) shows that in the momentum representation (where A has diagonal form) the measurement causes a multiplication of the wave function with a Gaussian amplitude of width $1/2\alpha$, which leads to a reduction of the wave function. For sufficiently low values of α , quantum mechanical phase coherence is not destroyed completely over one time step, so that quantum effects in the system behavior should be detectable by the measurement.

From (11) we can derive the statistics of the measurement results upon averaging over all measurement trajectories. A trajectory with given results $\tilde{A}^j := \{\tilde{A}(j'), 0 < j' \leq j\}$ has a differential probability measure $dP[\tilde{A}^j] = \prod_{j'=1}^j d\tilde{A}(j') p(\tilde{A}(j'))$. In the momentum representation with basis states $|n\rangle$, where

$$p|n\rangle = \hbar n|n\rangle, \quad A|n\rangle = a(n)|n\rangle, \quad (12)$$

we can express the probability density to measure a value $\tilde{A}(j)$ at the time $j\tau - \epsilon$, $\epsilon \searrow 0$, as

$$\begin{aligned} \bar{p}(\tilde{A}(j)) &= \int_{\mathbb{R}^{j-1}} dP[\tilde{A}^{j-1}] p(\tilde{A}(j)) \\ &= \sqrt{\frac{\alpha}{\pi}} \int_{\mathbb{R}} \bar{\rho}'(n, n; j) \\ &\quad \times \exp\left\{-\alpha [a(n) - \tilde{A}(j)]^2\right\} dn \end{aligned}$$

$$\text{with } \bar{\rho}'(n, n; j) := \langle n | \bar{\rho}'(j) | n \rangle = \overline{|\langle n | \psi'(j) \rangle|^2}. \quad (13)$$

Thereby one gets the relations

$$\overline{\tilde{A}(j)} = \overline{\langle A(j) \rangle'}, \quad (14)$$

$$\overline{\tilde{A}^2(j)} = \overline{\langle A^2(j) \rangle'} + \frac{1}{2\alpha} \quad (15)$$

for the connection between the statistics of the recorded quantity \tilde{A} and the system observable A . [$\langle A^m(j) \rangle'$ denotes the expectation value of A^m with respect to the state $|\psi(j)\rangle'$.] Their variances then are related by

$$\overline{\Delta \tilde{A}^2(j)} = \overline{\langle \Delta A^2(j) \rangle'} + \frac{1}{2\alpha}. \quad (16)$$

It is useful to note that the total variance of A , $\overline{\langle \Delta A^2 \rangle} = \text{Tr}(\bar{\rho} A^2) - [\text{Tr}(\bar{\rho} A)]^2$, can be decomposed into one term $\overline{\langle \Delta_q A^2 \rangle} = \overline{\langle \psi | A^2 | \psi \rangle} - \overline{\langle \psi | A | \psi \rangle}^2$ describing the averaged quantum mechanical A variance of the individual state vectors and one term $\overline{\Delta_s \langle A \rangle^2} = \overline{\langle \psi | A | \psi \rangle^2} - \overline{\langle \psi | A | \psi \rangle}^2$, which gives the stochastic variance of the individual A expectation values, i.e.,

$$\overline{\langle \Delta A^2 \rangle} = \overline{\langle \Delta_q A^2 \rangle} + \overline{\Delta_s \langle A \rangle^2}. \quad (17)$$

III. DYNAMICAL LOCALIZATION OF THE DRIVEN QUANTUM PENDULUM

A chaotic quantum system that is sufficiently simple to allow for extensive numerical simulations but sufficiently complex to describe some real experiments is given by the periodically driven quantum pendulum, the Hamiltonian of which can be written in dimensionless form as

$$H_S = \frac{p^2}{2} + k \cos(\theta + \lambda \sin 2\pi t) \quad (18)$$

[17,18,29]. Besides k (potential strength) and λ (driving amplitude), the above mentioned rescaled Planck constant \hbar is a third parameter of this quantum system.

In [17] and [18] we have discussed the behavior of the driven pendulum in the context of two physical realizations: the current-driven Josephson junction and atoms in a modulated standing light wave, respectively. The latter has been taken up in a recent experiment by Raizen and co-workers [22]. In the following we briefly review

the analysis of the isolated driven pendulum dynamics.

The basic phenomenon describing the classical behavior of the system [32] is the crossing of the nonlinear resonance at which $\dot{\theta} = p = -2\pi\lambda \cos 2\pi t$. Phase space points in the interval $|p| \lesssim 2\pi\lambda$ experience two crossings per period $T = 1$ and outside each crossing the pendulum is effectively free. [We will always assume that the width of the resonance ($4\sqrt{k}$) is much smaller than the range of its oscillations ($4\pi\lambda$). Otherwise one only will come to a rather narrow chaotic separatrix layer; the quantum dynamics in a chaotic separatrix layer were studied in [33].] Fourier transformation of (18) with respect to time yields a multiplet of stationary primary resonances at $p_m = 2\pi m$, $m \in \mathbb{Z}$, with widths $4\sqrt{k}J_m(\lambda)$ (J_m are the Bessel functions), which can be neglected for $|m| > \lambda$. Chirikov's resonance overlap criterion then leads to the condition

$$K := \frac{k}{\sqrt{\pi\lambda}} > K_C \approx 1 \quad (19)$$

for global chaos in the region $|p| \lesssim 2\pi\lambda$ [32].

If the rate of displacement of the moving resonance ($4\pi^2\lambda$) is much larger than the rate of change of the pendulum frequency (k), we speak of the case of fast crossing. The result of the crossing is then in a first approximation the same as that for a linear oscillator: the momentum p experiences a change by an amount of $\delta p \approx k/(\sqrt{2\pi\lambda}) \sin(\theta + \lambda \sin 2\pi t \pm \pi/4)$, where the sign is determined by the direction in which the resonance is passed [32]. Under the condition of global chaos the sequence of arguments of the sinus in the above expression is approximately random and distributed uniformly over the interval $[0, 2\pi)$. Thus the chaotic system spreads diffusively over the momentum region $|p| \lesssim 2\pi\lambda$, which is restricted by the Kol'mogorov-Arnol'd-Moser (KAM) tori beyond. Figure 1(a) displays a corresponding phase space plot numerically generated by the stroboscopic map of the canonical variables (θ, p) after each time period $T = 1$. The diffusion constant is given by

$$D \approx \frac{\overline{\delta p^2}}{T/2} \approx \frac{k^2}{2\pi\lambda}. \quad (20)$$

(The bar denotes the average with respect to the random resonant phases θ .) This increase in the momentum variance due to the kicklike resonance crossings is shown in Fig. 1(b), where we see reasonable agreement of the numerical simulation with the theory. After a time $t_s \approx 4\pi^2\lambda^2/D$ an ensemble of pendulums with initial momentum $p(0) = 0$ will reach a uniform distribution in the interval $p \in [-2\pi\lambda, 2\pi\lambda]$, i.e., stationary root mean square fluctuations $\sqrt{\Delta p^2} \approx 4\pi^2\lambda^2/3$.

In the case of a slow crossing resonance, where $4\pi^2\lambda/k \ll 1$, the chaotic diffusion constant cannot be derived in such a simple manner as above and is given by a more complex expression [32]. Furthermore, system points that lie initially within the separatrix of the resonance can follow the motion of the resonance; they build up a stable island oscillating in the chaotic sea. This type of motion is called phase locking [29,32]. We will

restrict our following analysis of the chaotic pendulum to the more accessible regime of fast crossing.

The quantum dynamics of the periodically driven pendulum is determined by its Floquet states $|\nu\rangle$, i.e., the eigenstates of the time-evolution operator over one driving period U_1 , which satisfy $U_1|\nu\rangle = e^{-i\omega_\nu}|\nu\rangle$. From the similarity of the above described chaotic behavior of the driven pendulum with that of the chaotic kicked rotor, which can be mapped onto a one-dimensional Anderson model [11,13], one can conjecture that in the chaotic region, all Floquet states are exponentially localized due to destructive quantum mechanical interferences of tran-

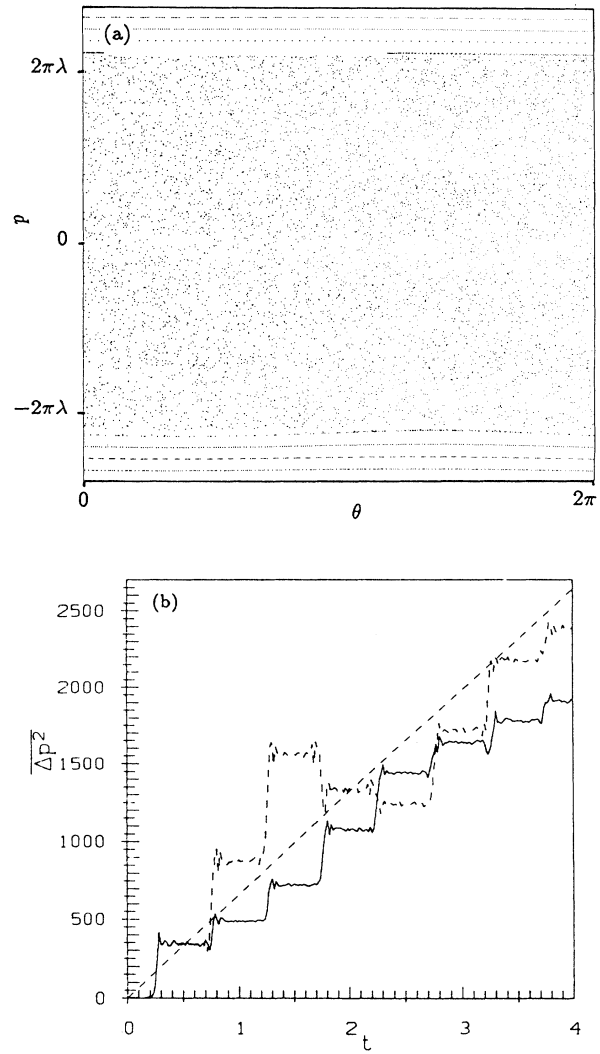


FIG. 1. Chaotic diffusion of the driven pendulum with $k = 594$ and $\lambda = 85$. (a) Phase space plot of the stroboscopic map of the canonical variables (θ, p) after each time period $T = 1$. (b) Momentum variance [for initially sharp momentum $p(0) = 0$] as a function of time. The solid curve shows results of a numerical simulation of the classical system, the dashed curve those of the quantized system with $k = 9.93$ (see below), and the other dashed line follows the theoretically expected increase with the diffusion constant (20).

sition amplitudes with large changes of n . According to this conjecture they take the form

$$|\langle n|\nu \rangle| \sim \exp\left(-\frac{|n - n_\nu|}{l}\right), \quad (21)$$

where l is the wave function localization length. So the spectrum of eigenphases ω_ν (quasienergies) is discrete. An initial state $|\psi(0)\rangle = |n = 0\rangle$, which is a superposition of about $2l$ Floquet states, spreads by classical diffusion for a time $t_D \approx 2l$. Then, if $t_D < t_s$, it develops into an exponentially localized distribution $|\langle n|\psi \rangle| \sim \exp(-|n|/l_D)$ with a dynamical localization length

$$l_D \approx 2l \approx \frac{D}{k^2} \approx \frac{k^2}{2\pi\lambda k^2} \quad (22)$$

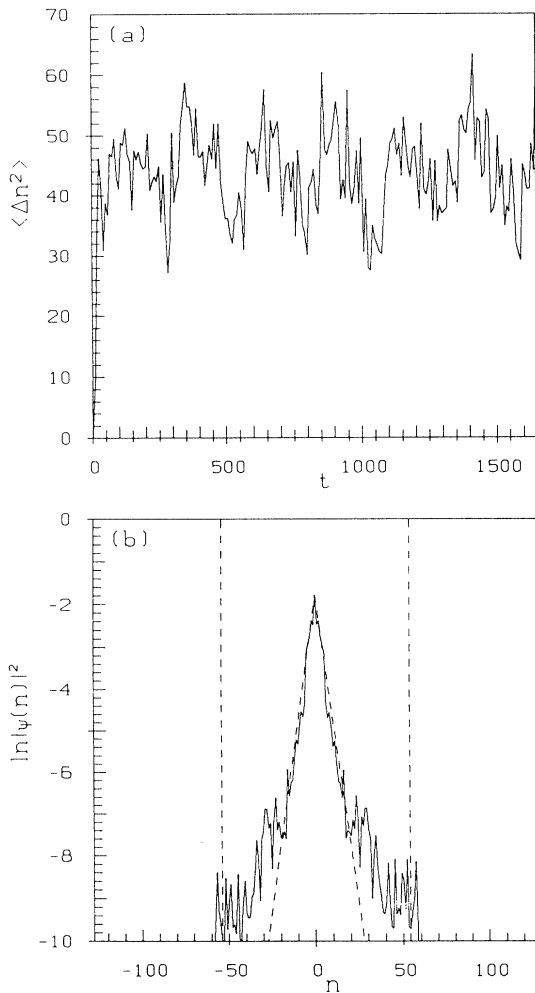


FIG. 2. Dynamical localization of the driven quantum pendulum with parameter values as in Fig. 1. (a) Variance of the momentum quantum number versus time. (b) Logarithm of the time-averaged n distribution. The dashed lines give the border $|n| = 2\pi\lambda/k$ of the classical chaotic domain and the exponential falloff with the rate $2/l_D$.

[34]. Thus, if $\lambda > \lambda_q := k/(2\pi\sqrt{k})$, the momentum fluctuations are quantum mechanically reduced to $\sqrt{\langle \Delta p^2 \rangle} \approx k l_D \sim 1/\lambda$. So they decrease inversely proportional to the driving amplitude λ as opposed to their classical increase proportional to λ , which can be found if $\lambda < \lambda_q$. First attempts to observe this effect of dynamical localization experimentally have recently been reported by Raizen and co-workers, who realized the driven pendulum by atoms in a modulated standing light wave [22].

Figure 2 shows the results of a numerical simulation already published in [17] to demonstrate the occurrence of dynamical localization. To get an effective computer algorithm we replaced the continuous time-dependent potential in (18) by a suitable periodic sequence of δ -function kicks like in (6). There the stroboscopic dynamics of the system can be studied by iterating a quantum map, which is obtained by exact integration of the Schrödinger equation over one kicking period τ . The relevant resonance structure remains unaffected if one chooses $\tau \ll 1, \lambda < 1/(2\tau)$ [32]. In the figure the initial sharp rise of the n variance by classical diffusion (also shown in Fig. 1) is followed by quasiperiodic fluctuations around a constant value, which is in good agreement with the square of the theoretically predicted dynamical localization length $l_D^2 \approx 45$. We also found the exponential falloff with a rate of $2/l_D$ in the time-averaged localized n -probability distribution displayed in Fig. 2(b).

In the regime of slow resonance crossing, which was also studied [29], the quantum analog to the above mentioned phase locking is realized by a motion, where the system follows the resonance along its adiabatic energy-bands. Superimposed on the oscillations due to the resonance movement, one then finds Bloch oscillations reflecting the periodic structure of the energy bands. Transitions from one band to another occur via Zener tunneling. This again results in an initially diffusive and later dynamically or adiabatically (i.e., by KAM tori) localized behavior. The simple estimates provided by dynamical localization theory are less accurate in this case, as in the case of fast crossing, because of the higher complexity of the underlying classical diffusion process [32] and the influence of the stable island around the oscillating resonance.

IV. DELOCALIZATION BY MEASUREMENT OF ANGULAR MOMENTUM

The effect of dynamical localization described above rests on quantum coherence. Thus the incoherent transitions of the system state due to the action of a measuring device discussed in Sec. II should lead to a delocalization.

A. Analytical estimates for the measured ensemble dynamics

To get an analytical picture of the mechanism of delocalization for a continuous measurement of the angular momentum we use the results of the preceding section and consider the chaotic driven pendulum in the

fast crossing regime as a kicked rotor with kicking period $T = 1$ and kicking strength $K = k/\sqrt{\pi\lambda}$. The borders of the chaotic region, i.e., the KAM tori at $|p| \gtrsim 2\pi\lambda$, can be viewed as acting like reflecting walls.

The measurement causes incoherent transitions between the Floquet states of the isolated system. The mean transition rate Γ defines a coherence decay time $t_c = 1/\Gamma$ as the mean lifetime of a Floquet state. If t_c is smaller than t_D , the time for establishing the localized behavior, the quantum coherences do not survive long enough and remain practically ineffective. Therefore, in this case of “strong coupling,” the classical diffusive spread in momentum space with the classical diffusion constant $D_{\text{cl}} := D/k^2 \approx l_D$ is also found for the quantum system. In the case of “weak coupling,” where $t_c > t_D$, the n variance can increase for $t > t_D$ on the time scale t_c by an amount of $D_{\text{cl}}t_D \approx l_D^2$. Hence we have a delocalization with a reduced (relative to the classical motion) diffusion constant

$$D_{\text{quant}} \approx D_{\text{cl}} \frac{t_D}{t_c} \approx \Gamma l_D^2. \quad (23)$$

Here the dynamical localization is reflected by the transition $D_{\text{cl}} \rightarrow D_{\text{quant}} < D_{\text{cl}}$ for $t > t_D$.

In order to calculate D_{quant} we have to determine the Floquet transition rate Γ for weak coupling between system and meter. For that purpose one can consider the nonselective (averaged over all measurement trajectories) time evolution of the measured system in first-order perturbation theory with respect to the coupling γ [4]. It follows from the master equation (5) with measured observable $A = n$. If we use the approximation of the driven pendulum by the kicked rotor described above, the master equation in the n representation can be integrated over one kicking period (with time cuts immediately before the kicks), yielding a stroboscopic map $\bar{\rho}(n', m'; j+1) = \sum_{n, m=-\infty}^{\infty} G(n', m'|n, m)\bar{\rho}(n, m; j)$ with a propagator

$$G(n', m'|n, m)$$

$$= \exp\left(-\frac{\alpha}{4}(n' - m')^2\right) U_1(n', n) U_1^\dagger(m, m'). \quad (24)$$

Up to first order in the coupling constant $\alpha = \gamma T = \gamma$ the propagator takes the form $G(n', m'|n, m) \approx U_1(n', n) U_1^\dagger(m, m') [1 - (\alpha/4)(n' - m')^2]$. For an estimate of the Floquet transition rate one has to change to the Floquet representation, where this first-order form can be written as

$$G(\nu', \mu'|\nu, \mu) \approx e^{i(\omega_\mu - \omega_\nu)} \left(\delta_{\nu\nu'} \delta_{\mu\mu'} - \frac{\alpha}{4} \sum_{n', m'=-\infty}^{\infty} (n' - m')^2 \times \langle \nu' | n' \rangle \langle n' | \nu \rangle \langle \mu | m' \rangle \langle m' | \mu' \rangle \right). \quad (25)$$

The decay rate of a Floquet state $|\nu\rangle$, $\Gamma =$

$[1 - G(\nu, \nu|\nu, \nu)]/T$, therefore is given by

$$\Gamma = \frac{\gamma}{2} \langle \nu | \Delta n^2 | \nu \rangle. \quad (26)$$

But the n variance of the exponentially localized Floquet states amounts to $l^2 \approx l_D^2/4$ (cf. Sec. III), so that $\Gamma = 1/t_c = \gamma l_D^2/8$. Inserting this result into the expression in (23) leads to a quantum diffusion constant

$$D_{\text{quant}} \approx \frac{\gamma}{8} l_D^4 \approx \frac{\gamma}{8} \frac{k^8}{(2\pi\lambda)^4 k^8} \quad (27)$$

for the case of weak coupling, where $t_c > t_D$, i.e., where the coupling constant α satisfies the relation

$$\alpha < \alpha_c \approx \frac{8}{l_D^3}. \quad (28)$$

Due to the existence of the borders of the chaotic region of the classical phase space at $|n| \approx \Delta n_{\text{ch}} := 2\pi\lambda/k$, the quantum diffusion will terminate after a time $t_s \approx t_D + (\Delta n_{\text{ch}}^2 - l_D^2)/D_{\text{quant}}$ with a stationary n variance

$$\overline{\langle \Delta n^2 \rangle}_s \approx \frac{\Delta n_{\text{ch}}^2}{3} = \frac{4\pi^2\lambda^2}{3k^2}. \quad (29)$$

A measurement of other observables instead of $A = n$ may imply Floquet decay rates that are not equal for all Floquet states. Then also other delocalization schemes (like a superdiffusive transient behavior) can be found [5,29].

B. Analysis via measurement trajectories

For an understanding of the mechanism of the quantum diffusion on the level of measurement trajectories of individual systems, we have to analyze the statistics in the n space by solving the appropriate stochastic Schrödinger equation. The widths of the individual stochastic wave functions, i.e., their quantum mechanical n variance $\langle \Delta_q n^2 \rangle$ and the stochastic variance of the n expectation values $\overline{\Delta_s \langle n \rangle^2}$, are of particular interest: The sum of these quantities results in the total n variance $\overline{\langle \Delta n^2 \rangle}$ [cf. (17)], which is expected to increase linearly in time for $t < t_s$, as we have seen above. In the following we are only concerned with the transient motion in the region $|n| < \Delta n_{\text{ch}}$, where $\overline{\langle \Delta n^2 \rangle} < \langle \Delta n^2 \rangle_s$.

Let us again approximate the action of the resonance crossings by δ -function-like kicks at times $t = j \in \mathbb{Z}$. According to the discussion in Sec. III, in the classically chaotic case, for times $t < t_D$, they lead to a diffusive spread of the wave function in the n representation with $D_{\text{cl}} \approx l_D$. Hence, for $0 < t < t_D$, due to each kick, $\langle \Delta_q n^2 \rangle$ increases by an amount of $\delta_n \approx D_{\text{cl}}T \approx l_D$. The expectation value $\langle n \rangle$ and the stochastic variance $\overline{\Delta_s \langle n \rangle^2}$ experience no direct influence of the kicks. So the total n variance $\overline{\langle \Delta n^2 \rangle} = \overline{\langle \Delta_q n^2 \rangle} + \overline{\Delta_s \langle n \rangle^2}$ also grows by $\delta_n \approx l_D$. As was discussed above, at $t > t_D$ quantum interferences can cause a reduction of the n diffusion constant and $\overline{\langle \Delta_q n^2 \rangle}$ and $\overline{\langle \Delta n^2 \rangle}$ merely increase by $\delta_n \approx D_{\text{qm}}T$ per

kick. Therefore the kicks then produce jumps in $\overline{\langle \Delta_q n^2 \rangle}$ and $\overline{\langle \Delta n^2 \rangle}$ of the form

$$\overline{\langle \Delta_q n^2 \rangle} \rightarrow \overline{\langle \Delta_q n^2 \rangle} + \delta_n, \quad \overline{\langle \Delta n^2 \rangle} \rightarrow \overline{\langle \Delta n^2 \rangle} + \delta_n,$$

with

$$\delta_n \approx \begin{cases} D_{\text{quant}} T \approx \frac{\alpha}{8} l_D^4, & \alpha < \alpha_c \\ D_{\text{cl}} T \approx l_D, & \alpha \geq \alpha_c \end{cases} \quad (30)$$

Away from the resonance crossings the system dynamic is well approximated by that of a free rotor under the influence of a continuous n measurement. For this case the corresponding stochastic Schrödinger equation of the nonlinear type (3) has the form

$$d|\psi\rangle = \left(-i \frac{k}{2} n^2 - \frac{\gamma}{4} (n - \langle n \rangle)^2 \right) |\psi\rangle dt + (n - \langle n \rangle) |\psi\rangle d\xi. \quad (31)$$

Using Ito calculus one can derive from (31) the stochastic differential equations for the first two moments of the quantum number of the angular momentum, outside the kicks,

$$\begin{aligned} d\langle n \rangle &= 2\langle \Delta_q n^2 \rangle d\xi, \\ d\langle n^2 \rangle &= 2(\langle n^3 \rangle - 2\langle n^2 \rangle \langle n \rangle + \langle n \rangle^3) d\xi, \\ d\langle \Delta_q n^2 \rangle &= -2\gamma\langle \Delta_q n^2 \rangle^2 dt \\ &\quad + 2(\langle n^3 \rangle - 3\langle n^2 \rangle \langle n \rangle + 2\langle n \rangle^3) d\xi. \end{aligned} \quad (32)$$

Since the Ito increment $d\xi$ is statistically independent of the preceding process and has a vanishing mean, we get outside the kicks

$$d\overline{\langle n \rangle} = 0, \quad d\overline{\langle \Delta n^2 \rangle} = 0. \quad (33)$$

The mean of the quantum mechanical n variance of the individual wave functions and the variance of their n expectation values satisfy the differential equations

$$\begin{aligned} d\overline{\langle \Delta_q n^2 \rangle} &= -2\gamma\overline{\langle \Delta_q n^2 \rangle^2} dt, \\ d\overline{\Delta_s \langle n \rangle^2} &= 2\gamma\overline{\langle \Delta_q n^2 \rangle^2} dt. \end{aligned} \quad (34)$$

For a system that initially is in an n eigenstate in the classically chaotic domain we can set the third cumulant (κ_3) in front of the Ito increment in the last equation of (32) approximately to zero. This is justified because, according to (9), the integration of the stochastic Schrödinger equation (31) results in a multiplication of the n distribution $|\langle n | \psi \rangle|^2$ with a Gaussian distribution and the diffusive action of the kicks can be represented by a convolution of the n distribution with a Gaussian function. Thus $|\langle n | \psi \rangle|^2$ keeps a nearly Gaussian form with vanishing higher cumulants ($\kappa_m, m > 2$). In (34) one can therefore replace $\overline{\langle \Delta_q n^2 \rangle^2}$ by $\overline{\langle \Delta_q n^2 \rangle}^2$ and thereby obtain a closed system of differential equations. The integration of these equations and those in (33) over one kicking period $T = 1$ and the consideration of the jumps (30) due to a kick then yield the following stroboscopic maps (with time cuts immediately before the kicks):

$$\overline{\langle n(j+1) \rangle} = \overline{\langle n(j) \rangle}, \quad (35)$$

$$\overline{\langle \Delta n^2(j+1) \rangle} = \overline{\langle \Delta n^2(j) \rangle} + \delta_n, \quad (36)$$

$$\begin{aligned} \overline{\langle \Delta_q n^2(j+1) \rangle} &= \overline{\langle \Delta_q n^2(j) \rangle} + \delta_n \\ &\quad - \frac{2\alpha \left[\overline{\langle \Delta_q n^2(j) \rangle} + \delta_n \right]^2}{1 + 2\alpha \left[\overline{\langle \Delta_q n^2(j) \rangle} + \delta_n \right]}, \end{aligned} \quad (37)$$

$$\begin{aligned} \overline{\Delta_s \langle n(j+1) \rangle^2} &= \overline{\Delta_s \langle n(j) \rangle^2} \\ &\quad + \frac{2\alpha \left[\overline{\langle \Delta_q n^2(j) \rangle} + \delta_n \right]^2}{1 + 2\alpha \left[\overline{\langle \Delta_q n^2(j) \rangle} + \delta_n \right]} \end{aligned} \quad (38)$$

with

$$\delta_n \approx \begin{cases} D_{\text{quant}} T \approx \frac{\alpha}{8} l_D^4, & \alpha < \alpha_c \\ D_{\text{cl}} T \approx l_D, & \alpha \geq \alpha_c \end{cases} \quad (39)$$

for $t > t_D$. Equations (35) and (36) express the quantum diffusion in the n space on the basis of quantities referring to the ensemble of all measurement trajectories. With the help of Eqs. (37) and (38) we can now look at the mechanism of the quantum diffusion on the level of individual measurement trajectories. First, the iteration of (37) leads to a stable fixed point at

$$\overline{\langle \Delta_q n^2 \rangle} = l_M^2 = \frac{\delta_n}{2} \left(\sqrt{1 + \frac{2}{\alpha \delta_n}} - 1 \right). \quad (40)$$

l_M describes the point of equilibrium between the two competing processes that determine the width of the wave function of the single system in the n representation: the increase of the width by the action of the kicks due to the underlying classical chaos and its reduction by the measurement. With (39) one can see that the reduction of the wave function indeed results in a width l_M that is smaller than l_D , the value for the isolated system. Second, if the system has reached the fixed point for the width of its wave function, the stochastic variance of its first n moment grows linearly like

$$\overline{\Delta_s \langle n(j+1) \rangle^2} = \overline{\Delta_s \langle n(j) \rangle^2} + \delta_n. \quad (41)$$

So the quantum diffusion is carried by the motion of the n expectation values alone, while the width of each wave packet is fixed at the constant value l_M . We therefore obtain the physical picture of individual wave packets with a reduced width l_M , which move diffusively through the n space.

In the case of strong coupling l_M becomes rather small and one obtains an effectively classical (chaotic) behavior with a diffusion constant $D_{\text{cl}} \approx l_D$. For weak coupling the measurement induced reduction of the width of the wave packets is less strong and the diffusion constant D_{quant} is lowered compared to D_{cl} by the influence of quantum interferences (i.e., a trace of the dynamical localization).

The reduction of the wave function, i.e., the quantity l_M , is hidden to an observer. However the quantum diffusion is reflected in the recorded measurement results. For \tilde{n} , which describes the time average of the n measurement signal over the period $\tau' = T/2$, we get, according

to (15) and (16),

$$\overline{\tilde{n}(j)} = \overline{\langle n(j) \rangle'}, \quad \overline{\Delta \tilde{n}^2(j)} = \overline{\langle \Delta n^2(j) \rangle'} + \frac{1}{2\alpha'} \quad (42)$$

with $\alpha' = \gamma\tau' = \alpha/2$. For the recorded \tilde{n} values one therefore also obtains a diffusive increase with the same diffusion constant as for the diffusive increase of n . The \tilde{n} variance in addition contains a superimposed constant contribution $(1/2\alpha')$ due to the inaccuracy of the measurement.

C. Numerical simulations

Figures 3–5 show the results of numerical simulations of the n measured chaotic quantum pendulum. They are based on measurement trajectories generated by a

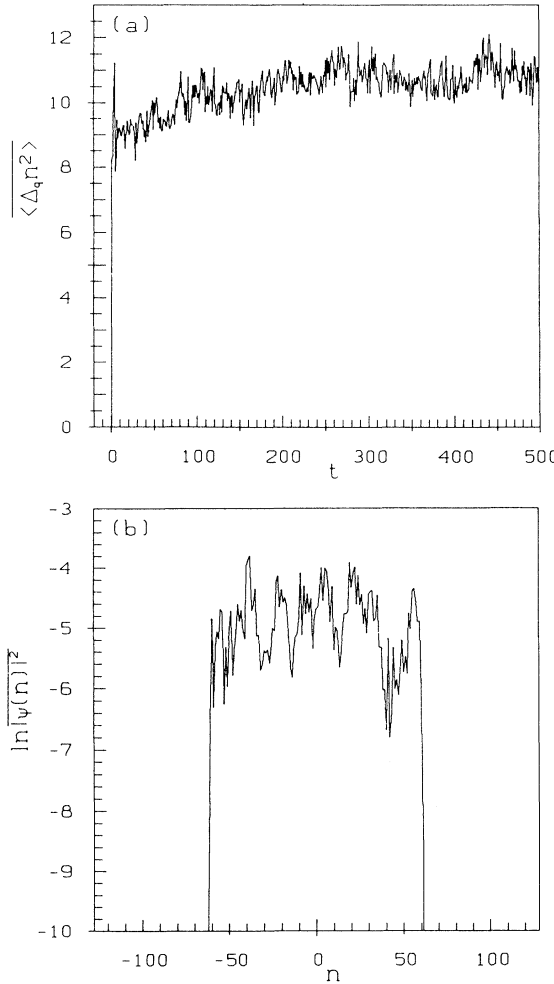


FIG. 3. Statistics in n space for the driven quantum pendulum with system parameters as in Fig. 1 and coupling to an n measurement with $\alpha' = 0.02$ (average of $N_T = 100$ measurement trajectories). (a) Variance of the momentum quantum number relative to the wave functions of individual measurement trajectories as a function of time. (b) Logarithm of the n distribution at time $t = 500$.

stochastic quantum map of the form (9)–(11) with time cuts at periodic intervals $\tau' = T/2 = 1/2$. The conservative part of the dynamic (originating from the unmeasured system) was implemented again with the help of the time discretization described in Sec. III.

Figure 3(a) displays the mean over 100 measurement trajectories of the n variance of the wave function as a function of time. It confirms the theoretically expected stationary value of $\langle \Delta n^2 \rangle_M^2 \approx 7$. The deviation between the numerical result and the analytical result (40) is of the order of $\delta_n \approx l_D$ and may be attributed to the assumption in (40) that the (chaotic) spread of the wave function takes place by δ -function-kicks with a period of $T = 1$,

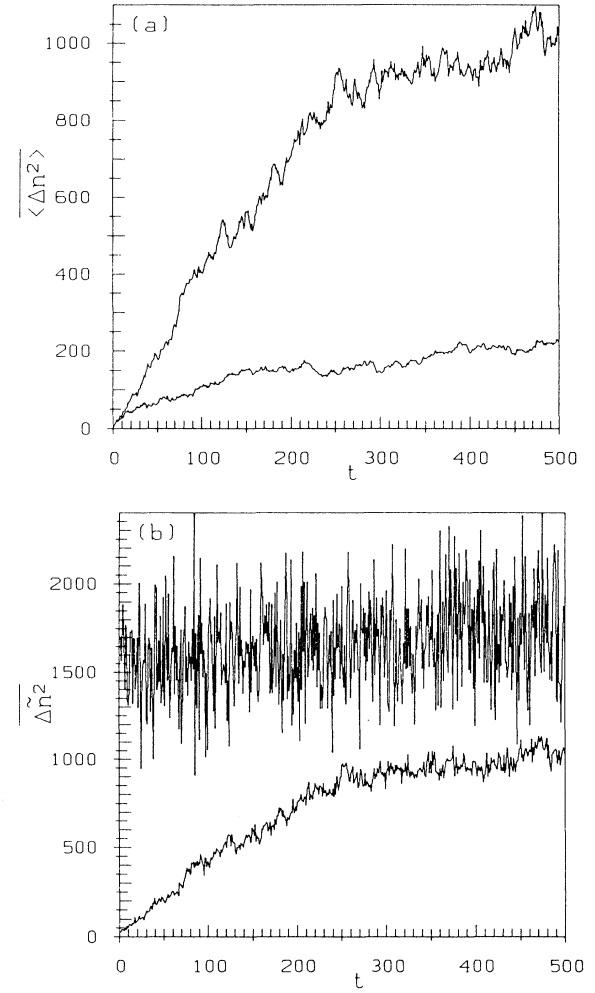


FIG. 4. Quantum diffusion of the driven pendulum with k , λ , and \hbar values as in Fig. 1. (a) Variance of the momentum quantum number relative to the statistical operator of the nonselective dynamics of the system. (b) Variance of the measurement results versus time. In the initially (on a coarse time scale) steeper curves it is $\alpha' = 0.02$ and the size of the ensemble of measurement trajectories is $N_T = 100$; in the shallower ones it is $\alpha' = 2 \times 10^{-4}$ and $N_T = 200$ [there we have displayed $\Delta \tilde{n}^2(t) - 1000$].

while in reality it happens due to the resonance crossings, twice per period T . Figure 3(b) shows the stationary distribution of the quantum number n over the classically chaotic region $|n| \leq \Delta n_{\text{ch}} = 54$, which may be roughly approximated by an equidistribution.

The initially (on a coarse time scale) steeper curves in Fig. 4 represent the time evolutions of the variances in n and \tilde{n} for this case of strong coupling. The nearly classical diffusion results in stationary values, which are in good agreement with the theoretical estimates of $\langle \Delta n^2 \rangle_s \approx \Delta n_{\text{ch}}^2/3 = 960$ and $\Delta \tilde{n}^2_s = \langle \Delta n^2 \rangle_s + 1/(2\alpha') \approx 985$, respectively. In the other example in Fig. 4 the parameter α' (i.e., the measurement accuracy) was reduced by a factor 100. Thus it belongs to the case of

weak coupling. It shows for $t > t_D \approx 7$ the expected slower quantum diffusion with a diffusion constant that is of the order of magnitude of the rough theoretical estimate $D_{\text{quant}} \approx (\alpha/8)l_D^4 = 0.1$. The lower accuracy of the measurement results is also reflected by larger statistical fluctuations in Fig. 4(b).

The scaling of the quantum diffusion constant with the dimensionless Planck constant \hbar is displayed in Fig. 5. The numerical values agree with the theoretically expected ones at least in order of magnitude. The latter are proportional to $1/\hbar^8$ and amount for the three examples shown from bottom to top to $D_{\text{quant}} \approx 0.1, 1.0, 4.3$, respectively.

V. CONCLUSIONS

In this work we have analyzed the behavior of individual chaotic quantum systems, namely, periodically driven pendula, under the influence of continuous measurements in time. Modeling the measuring device by a white quantum noise, which couples linearly to the system with a frequency-independent coupling constant, we have derived a Markovian quantum measurement process governed by a stochastic Schrödinger equation for the conditional time evolution of the state vector. For the special case of an angular momentum measurement of periodically kicked systems we have obtained from this an equivalent stochastic quantum map, which is very useful for numerical simulations of the measurement trajectories of chaotic quantum systems.

The isolated periodically driven pendulum was already studied in [17,18] in the context of physical realizations by current-driven Josephson junctions and atoms in a modulated standing light wave. In the regime of fast resonance crossing the effect of dynamical localization was there shown to occur. We have reviewed this work briefly in Sec. III.

A not necessarily perfect measurement of the angular momentum (or its quantum number n) produces a stochastic backaction on the state vector of the system and thereby causes at least a partial destruction of its quantum coherences. The latter are essential for a quantum interference effect such as dynamical localization to occur. Therefore repeated measurements of this kind lead to a delocalization of the classically chaotic quantum pendulum in the n space. In a theoretical analysis of this delocalization on the level of individual system states we have obtained the following picture: The single wave functions are reduced in their width in the n representation to a certain value that denotes the equilibrium between chaotic spreading and measurement induced shrinking. But their n expectation values then move diffusively until they fill more or less homogeneously the classically chaotic phase space region. Therefore one observes a transient linear increase of the total variance of n and of the recorded measurement results \tilde{n} .

For strong coupling between system and meter, i.e., for high measurement accuracy, the width in n of the individual wave functions becomes rather small and the diffusion takes place with the same diffusion constant as in

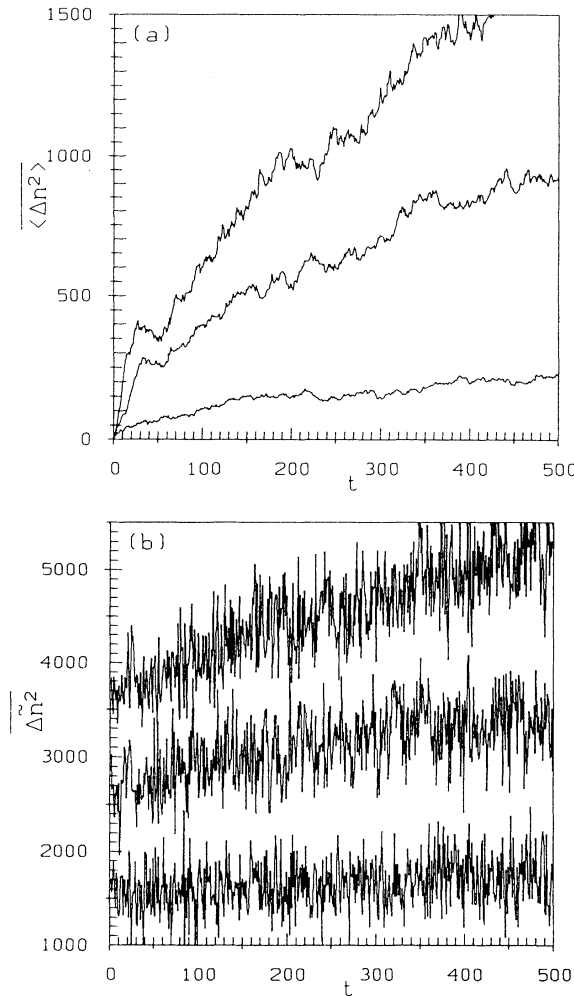


FIG. 5. Quantum diffusion of the driven pendulum with \hbar and λ values as in Fig. 1 and $\alpha' = 2 \times 10^{-4}$. (a) Variance of the momentum quantum number. (b) Variance of the recorded measurement results as a function of time (average over $N_T = 200$ measurement trajectories); from bottom to top \hbar takes the values $\hbar = 9.93, 7.45, 6.21$ [in the upper curve $\Delta \tilde{n}^2(t)$ is raised by 1000, in the lower curve it is lowered by 1000].

the classically chaotic case. A sufficiently strong coupling of the momentum observable to the meter would even destroy the correlations of the angular variable, which are always present in the classically regular case, and hence induce a diffusion in the n space even in the absence of classical chaos [5]. For weak coupling, however, the quantum diffusion only occurs in the classically chaotic case and may therefore serve as a signature of the underlying classical chaos. On the other hand, there remain, in this case, remnants of the quantum coherences, which reduce the quantum diffusion constant relative to the classical one. This can be interpreted as a trace of the dynamical localization of the isolated quantum system.

The rather rough analytical estimates are in agreement with the results of our numerical simulations, at least in order of magnitude. In particular we have shown that with decreasing rescaled Planck constant \hbar the measured chaotic quantum system passes over to the classical diffusive behavior quite rapidly.

The mechanism of the delocalization depends on the system observable that couples to the meter. For a measurement of n^m , $m > 1$, for example, the effective coupling constant increases with the quantum number of the excited n states. In the case of weak coupling, this leads to a transient superdiffusive behavior, which is followed by a diffusion with the classical diffusion constant [5,29].

The most promising possibility to see the delocalization of the quantum chaotic pendulum experimentally is given by the recent quantum optical realization [22], if one takes into account the coupling of the atoms to the electromagnetic environment and turns on the probability of spontaneous emissions by bringing the electromagnetic field sufficiently close to resonance with the atoms. Recent computer simulations of such cases [35,36] show a quantum diffusion similar to that discussed in the present work.

ACKNOWLEDGMENT

This work was supported by the Deutsche Forschungsgemeinschaft through its Sonderforschungsbereich 237.

APPENDIX

In this appendix we wish to derive the stochastic quantum map (9)–(11) for periodically kicked systems from the stochastic Schrödinger equation (1). For that purpose it is useful to write (1) in the Stratonovich form

$$d|\phi(t)\rangle = \left(-\frac{i}{\hbar} H_S - \frac{\gamma}{2} A^2 \right) |\phi(t)\rangle dt + A |\phi(t)\rangle \cdot d\xi(t),$$

where the Stratonovich product of two stochastic processes X and dY is defined as $X \cdot dY := X dY + \frac{1}{2} dX dY$. If now H_S is the Hamiltonian (6) of a τ -periodically kicked system and $A = A(p)$ an observable commuting with the momentum, one can integrate the above Stratonovich equation (as in the ordinary calculus) over one kicking period from $j\tau - \epsilon$ to $(j+1)\tau - \epsilon$, $\epsilon \searrow 0$,

yielding the linear stochastic quantum map

$$\begin{aligned} |\phi(j+1)\rangle &= \exp\left(\frac{[\Delta\xi(j+1)]^2}{2\gamma\tau}\right) \\ &\times \exp\left[-\frac{\gamma\tau}{2}\left(A - \frac{\Delta\xi(j+1)}{\gamma\tau}\right)^2\right] \\ &\times \exp\left(-\frac{i}{\hbar}\frac{p^2}{2}\tau\right) \exp\left(-\frac{i}{\hbar}V(\theta, j)\right) |\phi(j)\rangle, \end{aligned}$$

where $\Delta\xi(j+1) := \xi(j+1) - \xi(j)$. [Here we have used the abbreviation $f(j) := f(j\tau - \epsilon)$, $\epsilon \searrow 0$.] In this linear form the stochastic variables $\Delta\xi(j+1)$ are statistically independent and obey the Gaussian probability distribution

$$p_W(\Delta\xi(j+1)) = \frac{1}{\sqrt{\pi\gamma\tau}} \exp\left(-\frac{\Delta\xi(j+1)^2}{\gamma\tau}\right).$$

However, in order to get the proper statistical weight of the normalized physical state vector $|\psi\rangle = |\phi\rangle/\sqrt{\langle\phi|\phi\rangle}$ one has to use for $\Delta\xi(j+1)$ the distribution

$$p(\Delta\xi(j+1)) = \frac{\langle\phi(j+1)|\phi(j+1)\rangle}{\langle\phi(j)|\phi(j)\rangle} p_W(\Delta\xi(j+1))$$

(cf. Sec. II). From this we obtain the probability distribution of the quantities $\tilde{A}(j+1) := \Delta\xi(j+1)/(\gamma\tau)$ denoting the time average of the meter signal $A(t)$ over one kicking period τ ,

$$p(\tilde{A}(j+1)) = \alpha p(\Delta\xi(j+1))$$

with $\alpha := \gamma\tau$. Putting together the above results one gets the nonlinear stochastic quantum map for the normalized state vector $|\psi\rangle$,

$$\begin{aligned} |\psi(j+1)\rangle &= \frac{\left(\frac{\alpha}{\pi}\right)^{1/4} \exp[-\frac{\alpha}{2}(A - \tilde{A}(j+1))^2]}{\sqrt{p(\tilde{A}(j+1))}} \\ &\times |\psi'(j+1)\rangle \\ &= \frac{\left(\frac{\alpha}{\pi}\right)^{1/4} \exp[-\frac{\alpha}{2}(A - \tilde{A}(j+1))^2]}{\sqrt{p(\tilde{A}(j+1))}} \\ &\times \exp\left(-\frac{i}{\hbar}\frac{p^2}{2}\tau\right) \exp\left(-\frac{i}{\hbar}V(\theta, j)\right) |\psi(j)\rangle \end{aligned}$$

with

$$\begin{aligned} p(\tilde{A}(j+1)) &= \sqrt{\frac{\alpha}{\pi}} \langle\psi'(j+1)| \\ &\times \exp[-\alpha(A - \tilde{A}(j+1))^2] \\ &\times |\psi'(j+1)\rangle, \end{aligned}$$

which we used in Sec. II.

- [1] F. Haake, *Quantum Signatures of Chaos* (Springer, Berlin, 1991); M.C. Gutzwiller, *Chaos in Classical and Quantum Mechanics* (Springer, New York, 1990); L.E. Reichl, *The Transition to Chaos in Conservative Classical Systems: Quantum Manifestations* (Springer, New York, 1992).
- [2] E. Ott, T.M. Antonsen, Jr., and J.D. Hanson, Phys. Rev. Lett. **53**, 2187 (1984).
- [3] R. Grobe and F. Haake, Z. Phys. B **68**, 503 (1987).
- [4] T. Dittrich and R. Graham, Europhys. Lett. **4**, 263 (1987); **7**, 287 (1988); Ann. Phys. (N.Y.) **200**, 363 (1990).
- [5] T. Dittrich and R. Graham, Phys. Rev. A **42**, 4647 (1990); in *Quantum Chaos—Quantum Measurement*, edited by P. Cvitanović, I.C. Percival, and A. Wirzba (Kluwer, Dordrecht, 1992).
- [6] A.J. Lichtenberg and M.A. Lieberman, *Regular and Stochastic Motion* (Springer, New York, 1983).
- [7] J.A. Wheeler and W.H. Zurek, *Quantum Theory and Measurement* (Princeton University Press, Princeton, 1983).
- [8] P. Busch, P.J. Lahti, and P. Mittelstaedt, *The Quantum Theory of Measurement* (Springer, Berlin, 1991).
- [9] P.W. Anderson, Phys. Rev. **109**, 1492 (1958).
- [10] P.A. Lee and T.V. Ramakrishnan, Rev. Mod. Phys. **57**, 287 (1985).
- [11] S. Fishman, in *Quantum Chaos*, Proceedings of the International School of Physics “Enrico Fermi,” Course CXIX, edited by G. Casati, I. Guarneri, and U. Smilansky (North-Holland, Amsterdam, 1993).
- [12] G. Casati, B.V. Chirikov, F.M. Izrailev, and J. Ford, in *Stochastic Behavior in Classical and Quantum Hamiltonian Systems*, edited by G. Casati and J. Ford, Lecture Notes in Physics Vol. 93 (Springer, Berlin, 1979).
- [13] S. Fishman, D.R. Grempel, and R.E. Prange, Phys. Rev. Lett. **49**, 509 (1982); D.R. Grempel, R.E. Prange, and S. Fishman, Phys. Rev. A **29**, 1639 (1984).
- [14] B.V. Chirikov, F.M. Izrailev, and D.L. Shepelyansky, Sov. Sci. Rev. C **2**, 209 (1981); Physica D **33**, 77 (1988).
- [15] G. Casati, B.V. Chirikov, D.L. Shepelyansky, and I. Guarneri, Phys. Rep. **154**, 77 (1987).
- [16] R. Graham and M. Höhnerbach, Phys. Rev. A **45**, 5078 (1992).
- [17] R. Graham, M. Schlautmann, and D.L. Shepelyansky, Phys. Rev. Lett. **67**, 255 (1991).
- [18] R. Graham, M. Schlautmann, and P. Zoller, Phys. Rev. A **45**, R19 (1992).
- [19] J.R. Kuklinski, Phys. Rev. Lett. **64**, 2507 (1990).
- [20] E.J. Galvez, B.E. Sauer, L. Moorman, P.M. Koch, and D. Richards, Phys. Rev. Lett. **61**, 2011 (1988).
- [21] J.E. Bayfield, G. Casati, I. Guarneri, and D.W. Sokol, Phys. Rev. Lett. **63**, 364 (1989).
- [22] F.L. Moore, J.C. Robinson, C. Bharucha, P.E. Williams, and M.G. Raizen, Phys. Rev. Lett. **73**, 2974 (1994); J.C. Robinson, F.L. Moore, C. Bharucha, Q. Niu, R. Jahnke, G.A. Georgakis, Bala Sundaram, and M.G. Raizen (unpublished); P.J. Bardroff, I. Bialynicki-Birula, D.S. Krähmer, G. Kurizki, E. Mayr, P. Stifter, and W.P. Schleich (unpublished).
- [23] P. Pearle, Phys. Rev. A **39**, 2277 (1989).
- [24] N. Gisin, Helv. Phys. Acta **62**, 363 (1989); N. Gisin and I.C. Percival, J. Phys. A **25**, 5677 (1992).
- [25] L. Diósi, Phys. Lett. A **129**, 419 (1988).
- [26] H.J. Carmichael, *An Open Systems Approach to Quantum Optics* (Springer, Berlin, 1993).
- [27] H.M. Wiseman and G.J. Milburn, Phys. Rev. A **47**, 642 (1993); **47**, 1652 (1993).
- [28] V.P. Belavkin, J. Math. Phys. **31**, 2930 (1990); V.P. Belavkin and P. Staszewski, Phys. Rev. A **45**, 1347 (1992).
- [29] M. Schlautmann, thesis, Universität GH Essen, 1994 (unpublished).
- [30] P. Goetsch and R. Graham, Phys. Rev. A **50**, 5242 (1994); **51**, 3391(E) (1995).
- [31] C.W. Gardiner, *Quantum Noise* (Springer, Berlin, 1991).
- [32] B.V. Chirikov and D.L. Shepelyansky, Zh. Tekh. Fiz. **52**, 238 (1982) [Sov. Phys. Tech. Phys. **27**, 156 (1982)].
- [33] N. Bubner and R. Graham, Phys. Rev. A **43**, 1783 (1991).
- [34] D.L. Shepelyansky, Physica D **28**, 103 (1987).
- [35] S. Dyrting and G.J. Milburn (unpublished).
- [36] R. Graham and S. Miyazaki (unpublished).